Monitoring daily MLC positional errors using trajectory log files and EPID measurements for IMRT and VMAT deliveries

2014 Phys. Med. Biol. 59 N49

(http://iopscience.iop.org/0031-9155/59/9/N49)

IOP Publishing | Institute of Physics and Engineering in Medicine Physics in Medicine and Biology

Phys. Med. Biol. **59** (2014) N49–N63 doi:10.1088/0031-9155/59/9/N49

Note

Monitoring daily MLC positional errors using trajectory log files and EPID measurements for IMRT and VMAT deliveries

A Agnew[1], C E Agnew[1], M W D Grattan[1], A R Hounsell[1,2] and C K McGarry[1,2]

[1] Radiotherapy Physics, Northern Ireland Cancer Centre, Belfast Health and Social Care Trust, Northern Ireland, BT9 7AB, UK
[2] Centre for Cancer Research and Cell Biology, Queen's University Belfast, Belfast, Northern Ireland, BT9 7BL, UK

E-mail: adam.agnew@belfasttrust.hscni.net

Received 4 November 2013, revised 21 February 2014
Accepted for publication 7 March 2014
Published 15 April 2014

Abstract

This work investigated the differences between multileaf collimator (MLC) positioning accuracy determined using either log files or electronic portal imaging devices (EPID) and then assessed the possibility of reducing patient specific quality control (QC) via phantom-less methodologies. In-house software was developed, and validated, to track MLC positional accuracy with the rotational and static gantry picket fence tests using an integrated electronic portal image. This software was used to monitor MLC daily performance over a 1 year period for two Varian TrueBeam linear accelerators, with the results directly compared with MLC positions determined using leaf trajectory log files. This software was validated by introducing known shifts and collimator errors. Skewness of the MLCs was found to be 0.03 $\pm$ 0.06° (mean $\pm$1 standard deviation (SD)) and was dependent on whether the collimator was rotated manually or automatically. Trajectory log files, analysed using in-house software, showed average MLC positioning errors with a magnitude of 0.004 $\pm$ 0.003 mm (rotational) and 0.004 $\pm$ 0.011 mm (static) across two TrueBeam units over 1 year (mean $\pm$1 SD). These ranges, as indicated by the SD, were lower than the related average MLC positioning errors of 0.000 $\pm$ 0.025 mm (rotational) and 0.000 $\pm$ 0.039 mm (static) that were obtained using the in-house EPID based software. The range of EPID measured MLC positional errors was larger due to the inherent uncertainties of the procedure. Over the duration of the study, multiple MLC positional errors were detected

using the EPID based software but these same errors were not detected using the trajectory log files. This work shows the importance of increasing linac specific QC when phantom-less methodologies, such as the use of log files, are used to reduce patient specific QC. Tolerances of 0.25 mm have been created for the MLC positional errors using the EPID-based automated picket fence test. The software allows diagnosis of any specific leaf that needs repair and gives an indication as to the course of action that is required.

Keywords: EPID, trajectory log files, quality control, VMAT, truebeam

(Some figures may appear in colour only in the online journal)

1. Introduction

Intensity modulated radiation therapy (IMRT) and volumetric modulated arc therapy (VMAT) allow for the delivery of highly conformal dose distributions, using features such as dynamic multileaf collimators (MLCs), variable dose-rate, and, in the case of VMAT, variable gantry speeds. This allows for the creation of steep dose gradients, resulting in sharp contrasts between the dose delivered to the target and the dose delivered to organs at risk.

To gain the clinical advantage from IMRT and VMAT, it must be ensured that the treatment is planned and delivered accurately, while maximizing the resources that are available. A study performed on the clinical impact of implementing IMRT (Miles *et al* 2005), found that although there was a reduction in radiographer time per patient by almost 5 h, this was counteracted by an increase in medical physics time per patient by 5 h, of which a significant component was patient-specific quality control (QC). Guidelines for the development of IMRT suggested that individual patient-specific quality assurance (QA) measures should be carried out for at least the first ten patients to confirm delivery of the treatment plan (MacKay *et al* 2010). Reduced levels of patient-specific QC can be justified once the success of the initial implementation is verified via review although the amount of QC is still a debated topic (Siochi *et al* 2013).

If patient-specific QC is to be reduced, a comprehensive machine-specific QA program must be in place that ensures all parameters of the treatment are within tolerance. Although this machine-specific QA program will require additional resources initially, this will better accommodate an expanding service than a patient-specific orientated QA program. Patient-specific QC is restrictive as the time spent assuring plans will increase as the number of patients being treated increases.

As complex dose distributions are created using the MLCs, it is essential that the accuracy, and reproducibility, of the MLCs are routinely monitored to ensure that the actual positions of the MLCs during treatment correspond to the planned positions. LoSasso *et al* (1998) found that for dynamic treatments, a 0.5 mm systematic error in MLC position could potentially give a 5% dose error for a leaf gap of 10 mm. It has also been shown that a 3 mm random error in MLC positions could lead to a 0.7% change in average dose to a PTV (Betzel *et al* 2012). Budgell *et al* (2000) have shown that accurate dose delivery for IMRT fields require better than 1 mm accuracy of leaf position. ESTRO guidelines propose ± 0.5 mm as an acceptance criterion for MLC positioning accuracy for IMRT (Alber *et al* 2008).

Discrepancies between the planned and actual MLC positions, for Varian linear accelerators, could be a result of degradation of the performance of each motor, a loss of counts by the encoder, or a faulty or loose t-nut. Additional MLC errors could be a result of bank displacement (Rowshanfarzad *et al* 2012b, Rangel and Dunscombe 2009) and also

a rotational error in the treatment head (Rowshanfarzad *et al* 2012a). MLC errors can be inferred from dose deviations on film (Ling *et al* 2008), EPID (Chui *et al* 1996), and ionization chambers (LoSasso *et al* 1998). Log files that are created each time a dynamic delivery occurs can also be used to evaluate leaf positions (Litzenberg *et al* 2002).

A static gantry and a rotational gantry version of the test pattern 'picket fence test' (PF test) delivered to film or EPID can be used to assess the characteristics of the MLCs. These PF tests were analysed qualitatively using an image acquired on a film/EPID to assess for leaf gap errors of greater than 0.5 mm (Ling *et al* 2008). Automation of this analysis has previously been performed using cine portal images (Rowshanfarzad *et al* 2012a). Cine imaging is not available on all linear accelerators, including the Varian TrueBeam v1.5 and v1.6 which use integrated portal images. As well as a delivered test pattern being recorded on the EPID, log files that record MLC positions during the treatment can also be analysed. Previous studies have independently validated log file data using portal dosimetry (Stell *et al* 2004) and diode arrays (Li *et al* 2002) by inserting deliberate errors and assessing the ability of the method to detect them. Although log files are seen as a potential way to reduce patient specific QC and it has been suggested that they should be checked using independent imaging methods (Rowshanfarzad *et al* 2012a), as yet no longitudinal analysis of imaging and log files to quantitatively evaluate MLC errors has been carried out. This evaluation of leaf errors over time may lead to a better overview of the performance of individual leaves.

In-house software was developed to analyse MLC positions using an integrated electronic portal image. Results from over 800 test patterns delivered daily on two clinical Varian TrueBeams over a 1 year period were analysed. Analysing the delivery using both EPID and trajectory logs simultaneously provided an independent test to verify that the log files replicate the system accurately. Detailed analysis of MLC error detection is presented with suggested tolerances for MLC positional accuracy given.

2. Materials and method

All irradiations were carried out using two Varian TrueBeam v1.5 linear accelerators (Varian Medical Systems, Palo Alto, CA) operating at 6 MV (TrueBeam1 (TB1) and TrueBeam2 (TB2)). Each linac was matched and equipped with Millennium 120 leaf MLCs. Each bank of MLCs comprises 60 tungsten alloy leaves, of which the central 40 are 5 mm wide and the outer 20 are 10 mm wide (at isocentre). Images, integrated over the delivery were acquired in DICOM format with on-board Varian aS1000 EPID (active area 40 $\times$ 30 cm^2, 1024 $\times$ 768 pixels) attached to the linacs by an exact-type arm positioned at 140 cm source to detector distance.

2.1. Picket fence (PF) test

In the PF test, the MLC leaf pairs sweep across the field, irradiating a 1 mm gap every 15 mm. This test was delivered with the EPID positioned to record the response, as seen in figure 1, resulting in an image where the irradiated gaps were visible as ten stripes. This test allows for the evaluation of the leaf positions and the distance between opposing leaves. The PF was performed weekly with the gantry static at 0°, 90°, 180° and 270° (static PF), and daily while the gantry was rotating over 340° from 180° to 200°. The test pattern for the rotational PF was based on the pattern introduced by Ling *et al* (2008). As the collimator was at 0°, this tested the effects of gravity on the leaves. The *X* and *Y* jaws were used to collimate the beam to the sensitive area of the detector, resulting in leaf pairs 11 to 50 being visible on the EPID. This study concentrated on the inner leaves as the outer leaves are not used in the majority of

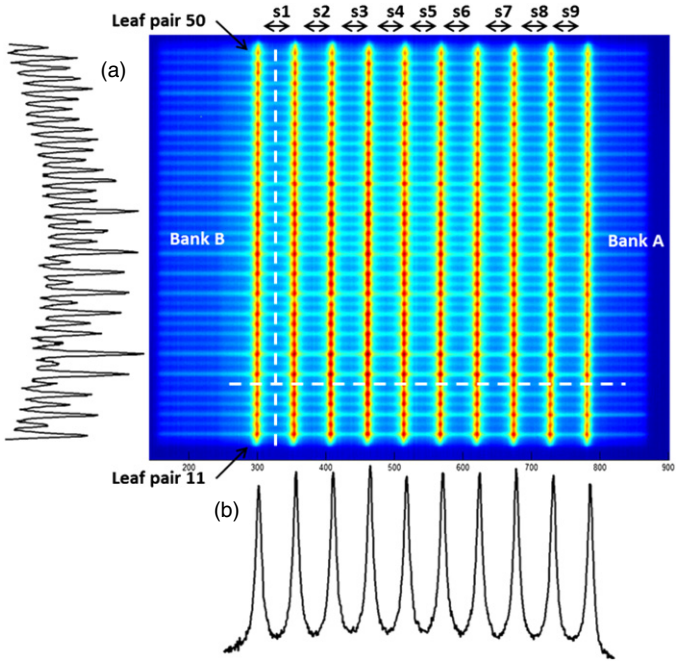

Figure 1. Picket fence test showing ten pickets (stripes), nine sub-sections (s1–s9), and profiles taken across (a) the leaves, and (b) the pickets.

treatments, although a variation of the test outlined in this study is used to evaluate outer leaf errors.

2.2. EPID picket fence software

In-house software, developed in Matlab vR2010a (The Mathworks Inc, Natick, MA), analysed the data acquired on the EPID images and determined the separation of the leaf gaps and the position of the gap for each stripe. From this, the average positions of each individual leaf on each bank were deduced relative to the positions at initial MLC calibration. The program also calculated the skewness of the leaf bank carriage and the offset of the MLC carriage with respect to the EPID at calibration. A skewed bank carriage could result in errors in dose delivery. Maximum pixel values for the stripes were used to calculate leaf separation and therefore the calibration between peak pixel value and leaf separation was required.

2.2.1. EPID calibration procedure. During MLC calibration, each leaf position is calibrated by driving the leaf until it breaks a light beam at a known position. Immediately following recalibration of the MLC, it was assumed that the MLCs are optimally positioned so this was used to create the PF calibration files, to which the leaf gap separations and positions were subsequently compared. Additional QC tests on the MLCs (IPEM 1999) are performed to ensure that any systematic errors initiated during the calibration process are kept to a minimum.

(i) *Separation of the leaf gaps.* To calculate the separation of each leaf gap, the central position of each leaf was required. The centre of each leaf was determined from a profile perpendicular to the movement of the leaves between each stripe (sub-section s1–s9)

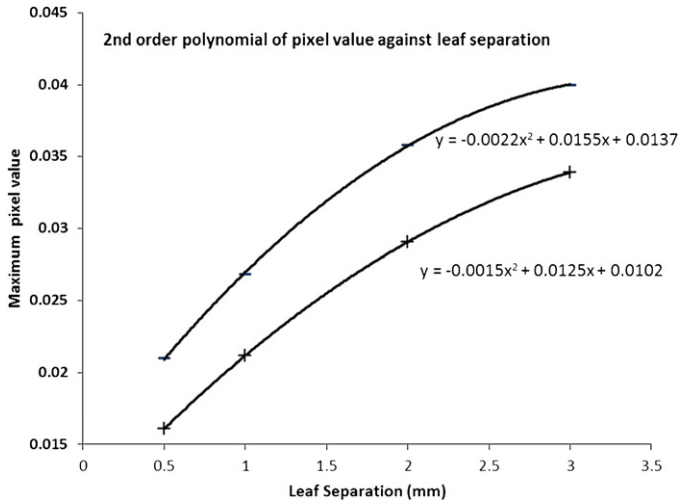

Figure 2. Examples (leaf50/stripe1 (+) and leaf30/stripe5 (−)) of the leaf separation against pixel value.

(figure 1, profile (a)). The positions of the minimum pixel values (a), which equate to the centre of each leaf pair, were acquired for each sub-section. The central position of each leaf was determined as the average of each minimum.

To determine the leaf separation a second profile was then created at the centre of each leaf pair in the direction of the motion of the leaves (figure 1, profile (b)). The leaf gap was recorded using the maxima along this profile.

To determine the width of the leaf separation, the relationship between the leaf separation and EPID pixel value was determined. The maximum pixel value was determined for known leaf separations of 0.5, 1, 2 and 3 mm. Increased leaf separation resulted in an increase in EPID pixel value as illustrated in figure 2. The relationship was fitted with a second order polynomial curve for each leaf pair at each stripe, with the a, b and c coefficients being saved as data files (figure 2). The sample separation against pixel value in figure 2 shows that individual calibration curves are required as the relationship between separation and pixel value varies between leaves and between stripes. This variation is the result of leaf 50 being situated at the beam edge and therefore is not at full scatter equilibrium. This variation also occurs for leaf 11, which is also at the beam edge. The maximum peak values were also saved in a data file. The errors in determining leaf positions as a result of this calibration step are estimated through the 95% confidence interval of ± 0.04 mm with a maximum error of less than ± 0.06 mm. These values were established through repeat PF measurements on the day of MLC re-calibration.

(ii) *Leaf pair positions.* The central position at each stripe in each leaf pair was determined. The full width half maximum (FWHM) for each leaf pair was found by utilizing the maximum and minimum values for the stripes and sub-sections in the 1 mm calibration PF. The midpoint of the FWHM values was taken as the central position of the leaf gap. These positions were saved as a data file and used as MLC reference positions during subsequent analysis.

2.2.2. EPID software analysis. When analysing PF tests, the separation width and leaf gap position were found with the same method used for the calibration files. As the leaf separations

were calculated using the maximum EPID pixel values, small deviations in the machine output affected the maximum EPID pixel values, and therefore the apparent leaf separation. An output correction was required to correct for this. The mean peak values (of all leaf pairs) of the delivered PF and the calibration PF were used to correct for deviations in the peak values due to variations in output between the calibration files and the delivered PF. (Output correction = average peak value PF/average peak value calibration file.)

This output correction was applied to each of the peaks in the delivered PF. Each peak value was then converted into a leaf pair separation, using the calibration curve.

The position of each centre of each leaf pair relative to the calibration files was calculated. Any effect of collimator skewness or EPID displacement was calculated and corrected. The skewness of the MLC bank with respect to the imager was found using the gradient of the leaf offsets against leaf distance from centre of rotation. The error in imager position was found by the average error of the centre of each leaf pair positions. This resulted in any error in the MLC positions being a factor of MLC position only. The centre of each leaf pair position was compared with the positions during the calibration.

Individual leaf positions for bank A and B were then calculated using the leaf pair separation and leaf pair positions. The average position of each leaf (over the ten stripes) was displayed, with any leaf falling outside the systems tolerance being highlighted. All leaf separations, leaf shifts, positional errors for bank A and B, skewness and offset are saved to file with trends over time investigated.

2.2.3. Validation of software. To validate the software, three types of errors were introduced into two leaves in the PF.

(i) *Leaf gap separation*. The separation between leaf pair 33 and 43 were changed from 1 mm to 0.5, 0.9, 1.5 and 2 mm by changing the position of leaf B in the pair. The altered PF tests were repeated on each clinical machine.

(ii) *Leaf pair offset.* Both leaves in selected leaf pairs were shifted in the same direction by 0.1, 0.5 and 1.0 mm. This test verified that the position of the leaves could be established when the separation remained the same.

(iii) *Collimator rotation effect on skewness*. It was found during this study that greater errors in the collimator angle could occur by manually positioning the collimator using the thumbwheel controller, rather than using the auto-position option available on the TrueBeam. This was corrected for in the analysis using the in-house software. Static PFs were delivered at collimator angles up to $\pm 0.6^{\circ}$ from the zero position (set using auto-position) to verify the algorithm can correctly identify rotation in the collimator. The difference between manual and automatic collimator positioning was quantified by comparing collimator rotation errors for five delivered static PF using both positioning techniques.

2.3. Trajectory log file analysis

Errors in each leaf and each bank were determined from trajectory log files. The planned (taken from DICOM file created during planning) and actual (deduced from the number of turns on the MLC motor) MLC leaf positions are recorded every 20 ms in the TrueBeam trajectory log files. As the leaves are stationary during the pickets, only one leaf position at each control point was analysed. In-house software that was previously validated (Agnew *et al* 2012) was used to analyse the PF tests. As there were minor adjustments made to the software, the software

Table 1. Results from the EPID and log files in the detection of intentional gap errors and leaf pair offsets, presented as the mean and SD over three measurements of two leaves for both units.

Mean detected error ± 1 SD (mm)	Introduced error (mm)				Mean error from expected ±1 SD (mm)
	−0.5	−0.1	0.5	1	
EPID	−0.495 ± 0.017	−0.108 ± 0.028	0.528 ± 0.034	1.028 ± 0.043	−0.013 ± 0.033
Trajectory logs	−0.506 ± 0.004	−0.107 ± 0.003	−0.493 ± 0.004	−0.994 ± 0.004	0.006 ± 0.003
Mean detected offset ± 1 SD (mm)	**Introduced offset (mm)**				**Mean error from expected ±1 SD (mm)**
	0.1	0.5	1		
EPID	0.110 ± 0.007	0.439 ± 0.017	0.883 ± 0.019		0.056 ± 0.052
Trajectory logs	0.103 ± 0.000	0.503 ± 0.002	1.004 ± 0.000		−0.003 ± 0.002

Table 2. Results of the software for the detection of intentionally inserted errors in the rotation of the collimator. Collimator was positioned using the auto-position function.

Set angle (degrees)	−0.6	−0.2	0	0.2	0.6
Calculated angle (degrees)	−0.591	−0.140	0.030	0.248	0.623
Difference (degrees)	−0.009	−0.060	−0.030	−0.048	−0.023

was re-validated for this study using the same positions used for the EPID in-house software validation.

2.4. Statistical analysis

Leaf position errors for both EPID and logs are presented as mean ± 1 standard deviation (SD). Tolerance levels for leaf position errors were determined as the range in the positions of the leaves when the leaves were operating optimally.

3. Results

3.1. Validation

The sensitivity of the in-house software to detect errors in leaf positions and leaf pair separation was tested by inserting intentional leaf gap errors into two leaf pairs. The PF containing the errors was delivered three times to each treatment unit and compared to an error-free PF plan. It can be seen from table 1 that the EPID analysis software identified gap errors with an accuracy of 0.03 mm and offset error to 0.06 mm for an offset less than 0.5 mm but this offset error increases as the offset increases.

PF test results acquired with collimator angles ranging from 359.4° to 0.6° are presented in figure 3. The gradient created from the offsets of each set of leaves is used to calculate the collimator skewness, and correct the positions of the leaves. Table 2 outlines the results from the intentionally skewed PF. It can be seen that the software can identify the rotation of the collimator to an accuracy of 0.06°.

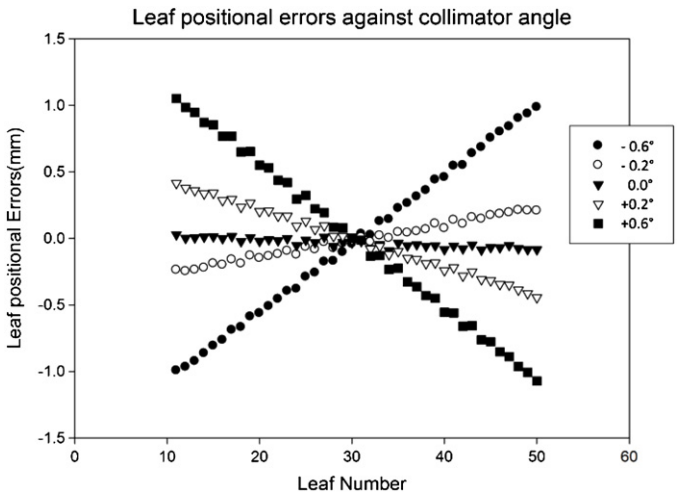

Figure 3. Effects of collimator rotation on leaf positional errors.

Table 3. Mean and SD for positional errors over 1 year for (a) rotational and (b) static PF tests.

(a) Rotational PF								
	EPID				Log file			
	TB1		TB2		TB1		TB2	
	A	B	A	B	A	B	A	B
Mean (mm)	−0.006	0.006	−0.002	0.002	0.006	0.001	0.007	0.002
SD	0.023	0.021	0.045	0.029	0.002	0.001	0.001	0.001
(b) Static PF								
	EPID				Log file			
	TB1		TB2		TB1		TB2	
	A	B	A	B	A	B	A	B
Mean (mm)	−0.002	0.002	0.003	−0.003	0.009	−0.001	0.009	−0.001
SD	0.035	0.030	0.050	0.041	0.011	0.010	0.010	0.010

3.2. EPID v log file analysis over time

Table 3 shows the mean ± 1 SD for positional errors over the study duration of 1 year for both units (TrueBeam1 and TrueBeam2), which resulted in over 800 deliveries. The mean positions are all within 0.01 mm of the expected position. It can be seen that the SD is much larger for the EPID data than for the log file data. This is consistent with the errors observed during the validation of the EPID and log file software. The SD for the EPID results for TB2, bank A for both rotational and static PF is larger than the other EPID banks as a result of a sub-optimal leaf. With the data for this leaf removed, the SD for this bank reduces to 0.03 and 0.04 mm for the rotational and static PF respectively, which is comparable to the other EPID results.

For the rotational PF the SD is smaller in both the EPID and log files compared to the static delivery. To allow for the rotational PF to be delivered over a 340° gantry rotation, MLC

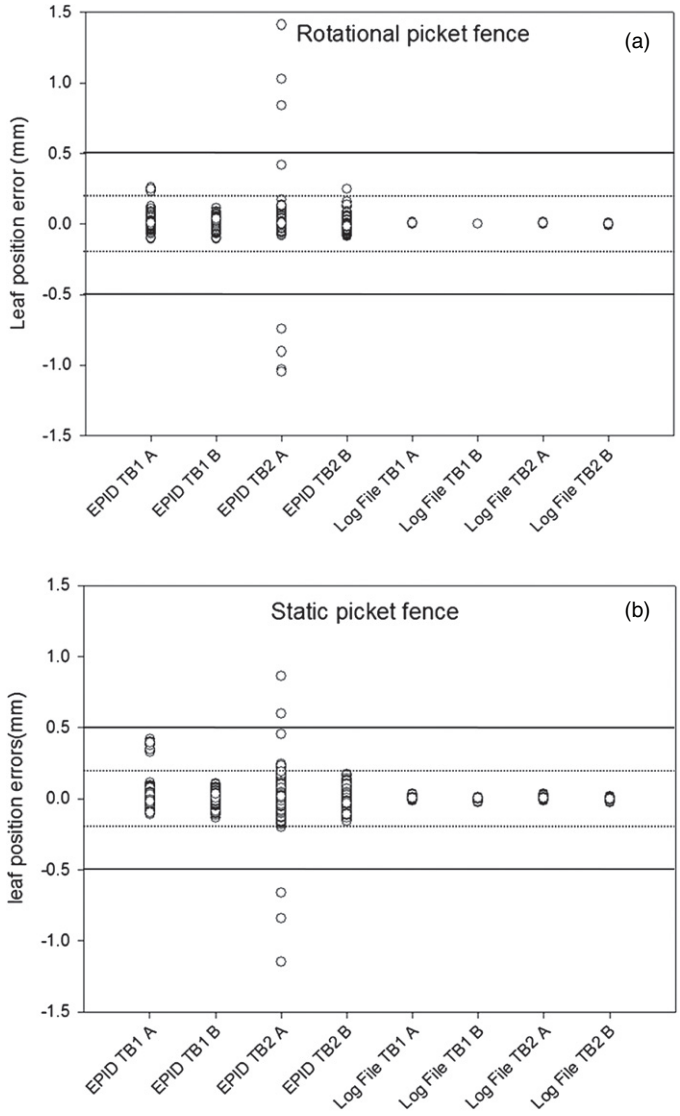

Figure 4. Positional errors for each leaf over 1 year period for two clinical TrueBeams (TB1 and TB2)), for both (a) static and (b) rotational PF tests. A and B in the horizontal axis represent leaf banks A and B. Ling *et al* (2008) suggested tolerance—solid line, proposed tolerance—dashed line.

speeds are reduced from 2.1 cm s^{-1} for static to 1.3 cm s^{-1} for rotational. This reduction in speed could have an effect on the positional accuracy of the MLCs (Wijesooriya *et al* 2012).

Figure 4 shows the leaf positional errors over the 1 year period along with the quantitative tolerance of 0.5 mm that was suggested by Ling *et al* (2008). A quantitative tolerance of 0.25 mm is also shown as a dashed line as any leaves that were outside this tolerance on a given day were investigated. Figure 4 shows that the error on leaf 28, bank A, TB1 would have been within a 0.5 mm tolerance and may not have been picked up by qualitative methods. It also shows that when the leaves are operating optimally, as is the case in TB1 and TB2, bank

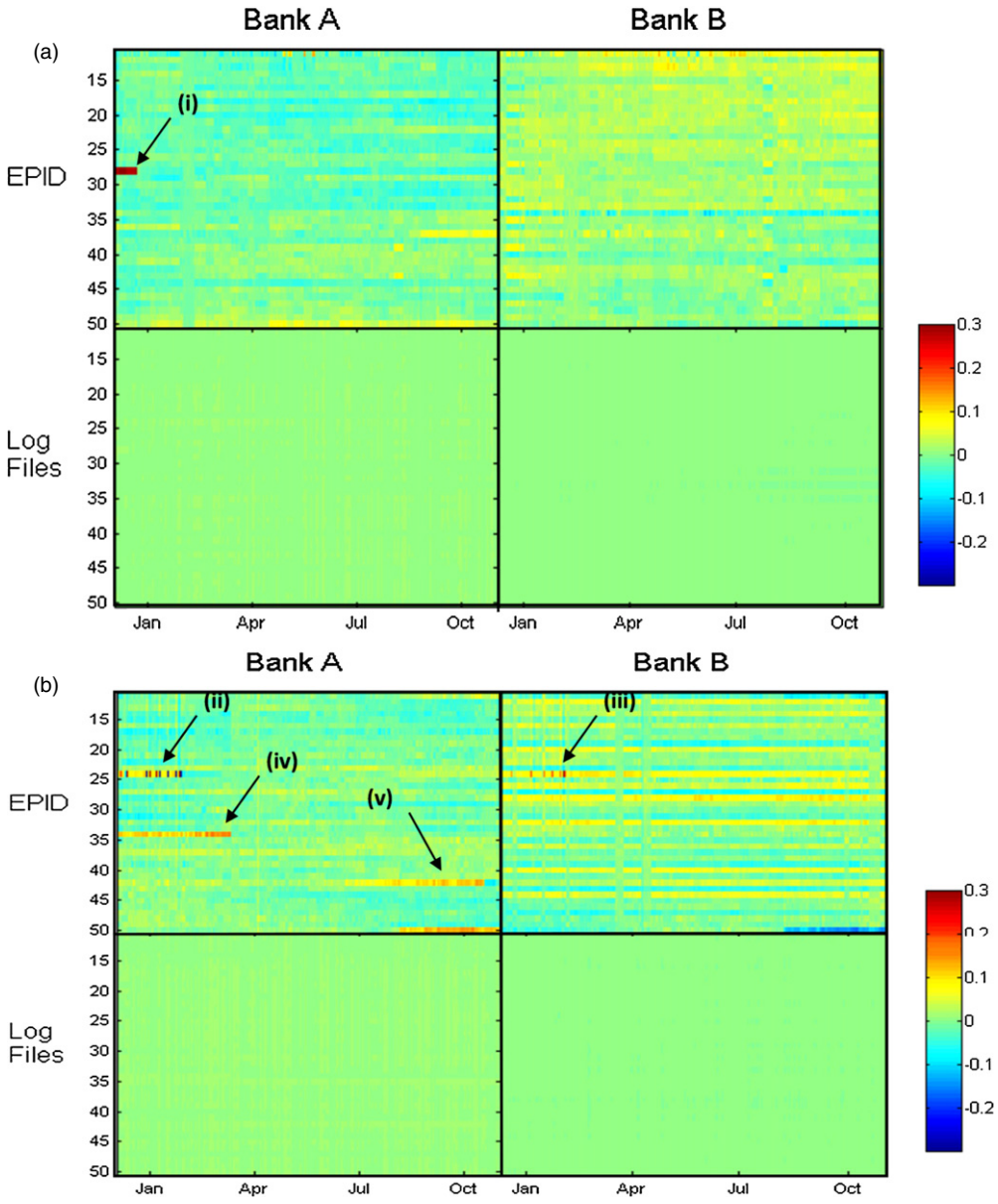

Figure 5. Leaf position errors over time for TB1 (a) and TB2 (b), analysed using both EPIDs and trajectory logs. *X*-axis represents time, *Y*-axis represents the leaf number, ranging from 10 to 50, and *Z*-axis (colour scale) represents the error in position.

B, all leaves lie within the tighter tolerance. The value of the static PF in combination with the rotational PF, as this error in TB1, bank A is also evident from this figure.

Errors in individual leaf positions were plotted using a colour-plot over time. It can be seen in figure 5(a), that a large leaf error of greater than 0.3 mm is present for leaf 28, bank A, of TB1 (figure 5(i)). This positional error is not present on the log file analysis. The magnitude of the leaf error remained constant over 10 days. Leaf 24 bank A, TB2 also had large positional errors according to the EPID data (figure 5(ii)). Again, this cannot be observed

Table 4. The effect of collimator positioning method on collimator angle and collimator rotation over the duration of the study.

	Manually		Automatically		All PF tests (Auto.)
	Max	Min	Max	Min	(Mean ± 1 SD)
Collimator angle error (deg)	0.173	−0.173	0.043	−0.043	0.03 ± 0.06

in the log file analysis. Both of these errors were corrected by replacing the motor and t-nut on the corresponding leaf, which corresponded to the error not being visible on the colour map. EPID results also showed smaller positional errors in leaf 28, bank B, TB2 (figure 5(iii)). These errors occurred when large errors on opposing leaf position caused the bank A leaf to influence the position of the bank B leaf. This was corrected when the motor and t-nut on the opposing leaf were replaced. Leaf 35, bank A, TB2 (figure 5(iv)), trended towards an increase in positional error over time although it was corrected after a recalibration of the MLCs.

Figure 6 shows the errors in the four leaves that were identified as a result of errors viewed in the PF test EPID results. The positions of each leaf were plotted over time for both EPID and trajectory logs. The graph also highlights when each leaf was repaired. Figure 6(a) shows the leaf in TB1 had a reproducible error of approximately 0.3 mm until motor and t-nut replacement returned the leaf to optimal operation. Leaf 28 on TB2 also had large deviations from the planned positions of between −1 and 1.5 mm for figure 6(b). Figures 6(c) and (d) shows that leaf 34 and 42 on TB2 drifted out of tolerance over a month and were corrected by calibrating the MLCs and replacing a t-nut respectively. Larger errors were observed for the static PFs than on the rotational PFs for the trending errors observed in leaves 34 and 42. None of the described positional errors were detected from the log file results and the leaves appeared to be working optimally over the study duration.

3.3. Collimator rotation errors

Static PF tests were delivered with the collimator positioned both manually and automatically. The results from table 4 show that automatically positioning the collimator results in more accurate collimator positions. The mean (± SD) over the study was found to be 0.03 ± 0.06°.

4. Discussion

In this study it was found that the trajectory logs created during the delivery of a PF test did not detect leaf positional errors that were detected using an EPID. This study has investigated this by analysing daily PF tests delivered to Varian TrueBeam linacs over a 1 year period. It was found that the average positions of the leaves calculated using both methods agreed although errors were detected using the EPID method which were due to re-calibration requirements, wear and tear of the t-nut or sub-optimal motor performance.

The in-house EPID software was validated using PFs with known separation and shift errors. The mean positional errors for the rotational and static PF over 1 year were found to be similar for EPID and log files. This study shows that the SD for the EPID data was greater than that of the log file data. This was due to the larger uncertainties in the calculation of the positional errors using the EPID. The SD was also greater for the static PF than for the rotational PF for both the EPID and the log files. This may have been a result of the increased leaf speed in the static PF. These SDs agree with the published results on EPID based QC

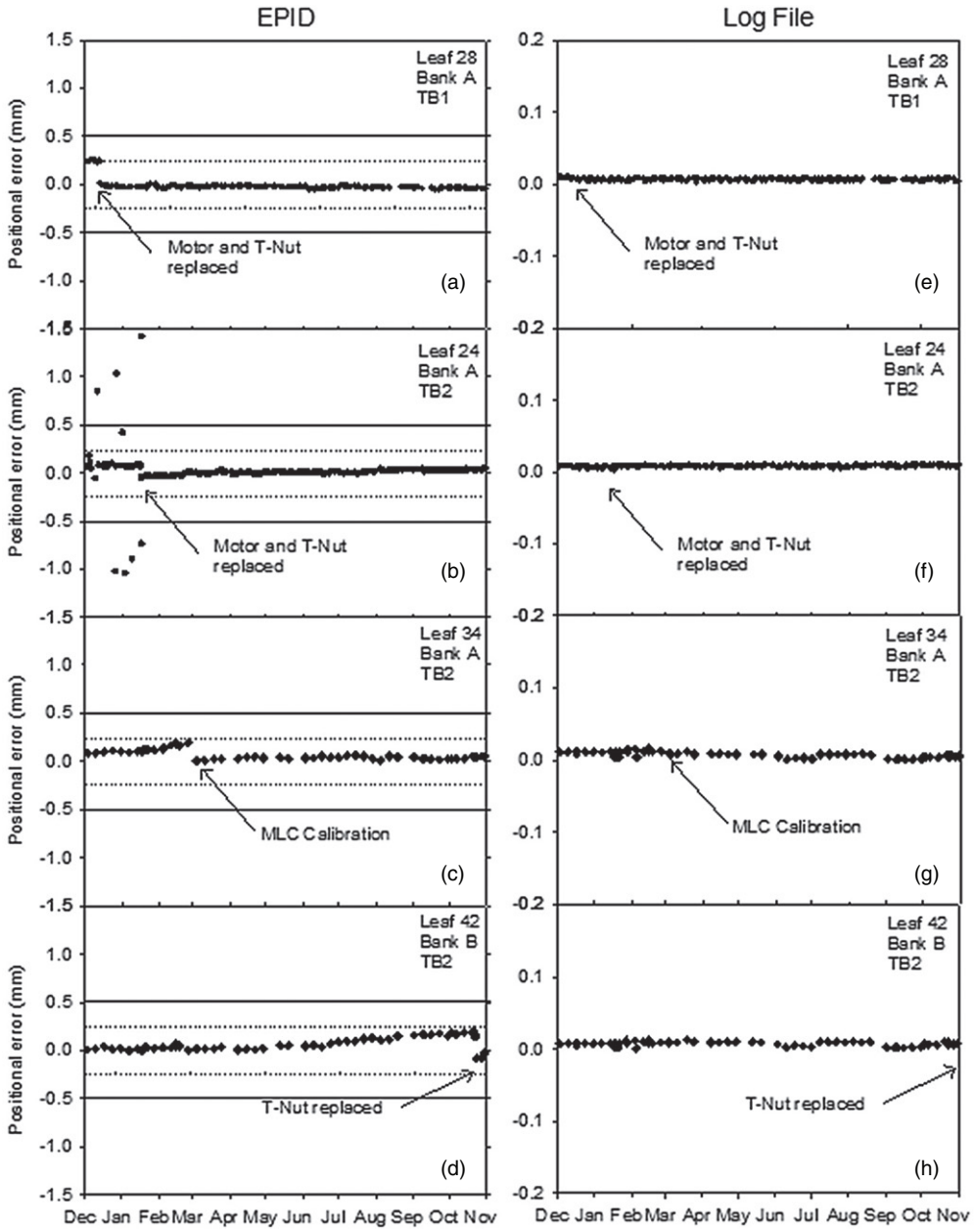

Figure 6. Sub-optimal leaves over time for EPID (a)–(d) and trajectory logs (e)–(h).

for positional errors of 0.02–0.03 mm (static) and 0.02 mm (rotational) (Rowshanfarzad *et al* 2012a) and 0.04 mm (rotational) (Jorgensen *et al* 2011).

Leaf errors on the two linacs were detected by the EPID over the course of the study. These errors were not identified in the log files and were outside the delivery tolerances of 0.2 mm set on the treatment units as determined by the EPID. The difference in the results from the EPID and log files could be due to the way the trajectory logs record the leaf positions

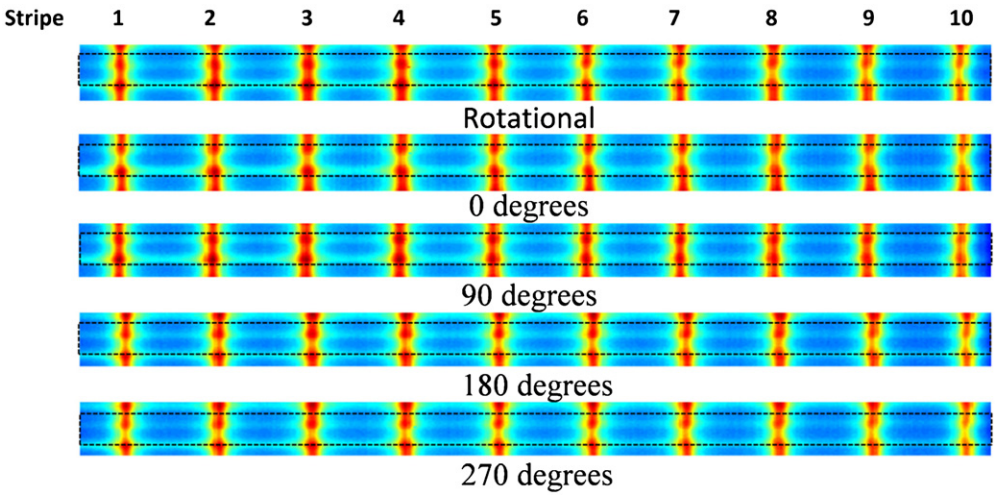

Figure 7. TB1, Bank A, leaf 28 at different gantry angles.

as the number of turns performed by the motor. If a t-nut is loose or broken, the position of the leaf relative to the motor could change, resulting in a read-out from the motor that does not correspond to the position of the leaf. This occurs in the example shown in figure 7, where during the rotational PF, leaf errors (stripes are not continuous) are only present in stripes 6–10, which correspond to gantry travel from 350° to 200° and the leaf position appears to change with gantry angle. Further analysis showed the error to be across all stripes for static PFs at 0°, 180°, 270° but not visible at 90°. This could have resulted in discrepancies between the EPID and the trajectory log files. As errors greater than stated in the ESTRO guidelines (Alber *et al* 2008) developed not only over weeks, but also over days, it is not adequate to periodically assess MLC position accuracy, but it is necessary to continuously monitor the MLCs on a daily basis.

Deliberate errors of between $\pm 0.6°$ of collimator rotation were delivered on the units. This verified the ability of the software to detect collimator rotation. It was shown that positioning the collimator manually can introduce errors in the collimator angle that would not be present when the collimator is positioned using the automatic position function on the treatment unit. This would suggest that 'plan based' QC, where the positions are pre-programmed, and therefore auto-position can be used, may be preferable to 'service mode' QC where manual movements are more common. Mean and SD for collimator rotation were found to be well within tolerance of 0.5° (Alber *et al* 2008), but it is important that they were accounted for in analysing MLC positions.

Log files remain a powerful tool to ensure that treatment plans are transferred to the linac correctly and can give a detailed picture of the performance of MLCs (Agnew *et al* 2012). However, this study shows that they should not be solely relied upon for QC as they do not always detect systematic machine faults. Therefore a robust measurement based machine-specific QA program is required before reducing the number of patient specific QC tests in IMRT or VMAT.

The PF test, performed daily as a rotational and stationary test with collimator 0, will test that each leaf is working optimally and test for the effects of gravity on the leaves. Taking into account all the QC results presented in this paper, tolerance levels of ± 0.25 mm have been established for the MLC positional errors detected using the EPID and quantitatively analysed

using the in-house software. This is comparable to other suggested tolerances of ± 0.3 mm (Jorgensen *et al* 2011) and ± 0.2 mm (Van Esch *et al* 2004). This is tighter than the tolerance of ± 1 mm and ± 0.5 mm suggested by AAPM (Klein *et al* 2009) and ESTRO (Alber *et al* 2008) respectively when the positions are analysed qualitatively. However, this study found, from quantitative automated analysis, that when the leaves are performing optimally, that the leaves should operate within this tighter tolerance.

5. Conclusion

It has been demonstrated, for the first time, that trajectory log files may not detect errors in multi leaf collimator (MLC) position due to t-nut or motor faults. If software based checks are being used as quality control (QC) tools, extensive measured machine-specific QC must be carried out. Tolerances of ± 0.25 mm have been created for the MLCs in the PF test using the EPID.

References

Agnew C E, King R B, Hounsell A R and McGarry C K 2012 Implementation of phantom-less IMRT delivery verification using Varian DynaLog files and R/V output *Phys. Med. Biol.* **57** 6761–77

Alber M *et al* 2008 *ESTRO Booklet No 9: Guidelines for the Verification of IMRT* (Brussels: ESTRO)

Betzel G T, Yi B Y, Niu Y and Yu C X 2012 Is RapidArc more susceptible to delivery uncertainties than dynamic IMRT *Med. Phys.* **39** 5882–90

Budgell G J, Mott J H, Williams P C and Brown K J 2000 Requirements for leaf position accuracy for dynamic multileaf collimators *Phys. Med. Biol.* **45** 1211–27

Chui C S, Spirou S V and LoSasso T 1996 Testing of dynamic multileaf collimation *Med. Phys.* **23** 635–41

IPEM 1999 Physics aspects of quality control in radiotherapy *Report no* 81 (York: IPEM)

Jorgensen M K, Hoffmann L, Petersen J, Praegtegaard L and Hansen R 2011 Tolerance levels of EPID-based quality control for volumetric modulated arc therapy *Med. Phys.* **38** 1425–34

Klein E E, Hanley J and Bayouth J 2009 Task Group 142 report: quality assurance of medical accelerators *Med. Phys.* **36** 4197–212

Li J G, Dempsey J F, Ding L, Liu C and Palta J R 2002 Validation of dynamic MLC-controller log files using a two-dimensional diode array *Med. Phys.* **30** 799–805

Ling C C, Pengpeng Z, Archambault Y, Bocanek J, Tang G and LoSasso T 2008 Commissioning and quality assurance of Rapidarc radiotherapy delivery system *Int. J. Radiat. Oncol. Biol. Phys.* **72** 575–81

Litzenberg D W, Moran J M and Fraass B A 2002 Verification of dynamic and segmental IMRT delivery by dynamic log file analysis *J. Appl. Clin. Med. Phys.* **3** 63–72

LoSasso T, Chen-Shou C and Ling C 1998 Physical and dosimetric aspects of a multileaf collimation system used in the dynamic mode for implementing intensity modulated radiotherapy *Med. Phys.* **25** 1920–7

MacKay R I, Staffurth J, Poynter A and Routsis D 2010 UK guidelines for the safe delivery of intensity-modulated radiotherapy *Clin. Oncol.* **22** 629–35

Miles E A, Clark C H and Urbano M 2005 The impact of introducing intensity modulated radiotherapy *Radiother. Oncol.* **77** 241–6

Rangel A and Dunscombe P 2009 Tolerances on MLC leaf position accuracy for IMRT delivery with a dynamic MLC *Med. Phys.* **36** 3304–9

Rowshanfarzad P, Sabet M, Barnes M P, O'Connor D J and Greer P B 2012a EPID-based verification of the MLC performance for dynamic IMRT and VMAT *Med. Phys.* **39** 6192–207

Rowshanfarzad P, Sabet M, O'Connor D J and Greer P B 2012b Investigation of the sag in linac secondary collimator and MLC carriage during arc therapies *Phys. Med. Biol.* **57** N209–24

Siochi R A, Molineu A and Orton C G 2013 Patient-specific QA for IMRT should be performed using software rather than hardware methods *Med. Phys.* **40** 070601

Stell A M, Li J G, Zeidan O A and Dempsey J F 2004 An extensive log-file analysis of step-and-shoot intensity modulated *Med. Phys.* **31** 1593–602

Van Esch A, Depuydt T and Huyskens D 2004 The use of a Si-based EPID for the routine absolute dosimetric pre-treatment verification of dynamic IMRT fields *Radiother. Oncol.* **71** 223–34

Wijesooriya K, Aliotta E, Benedict S, Read P, Tyvin R and Larner J 2012 RapidArc patient specific mechanical delivery accuracy under extreme mechanical limits using log files *Med. Phys.* **39** 1846–53